REFRACTION AND ATTENUATION IN THE TROPOSPHERE

Electromagnetic energy, often referred to in communications as *the signal* and traced in diagrams as a *ray,* travels at the speed of light, c, when in a vacuum, whether in the form of X rays, visible light, or a radio wave. The value of c is 3×10^8 m/s. When the signal passes through a medium that is not a vacuum, it travels more slowly. The ratio between c and the speed in the medium, v, is the *refractive index* of the medium, denoted by $n = c/v$. The refractive index of a medium does not just affect the speed of electromagnetic energy flowing through it; it can also cause the magnitude of the signal to fluctuate over time periods on the order of a second or longer due to variations in the refractive index within the medium. These signal fluctuations, called *scintillations,* are usually small and approximately symmetrical about the average level of the signal, although this is not always so in severe scintillations. Where two dissimilar media form a common boundary, the different refractive indices of the media will cause the signal direction to diverge from its path if the incident direction is not normal to the boundary. This is called *refraction,* and the incident and refracted directions either side of the boundary are given by Snell's law (e.g., Ref. 1).

The average refractive index of a medium is called the *bulk* refractive index, and it affects the average direction of the electromagnetic energy. Most media are not completely homogeneous, however: small volumes of different refractive indices will exist within the larger scale of the medium. These variations, which can exist over dimensions as small as a few centimeters in the troposphere, are termed the *small-scale* refractive index variations of the medium. They are like bubbles of air in a glass of soda. In the troposphere, the mixing of the small-scale "bubbles" within the larger scale of the medium can be caused by convection currents, due to heating of the air by the ground, or by turbulent effects in wind shear aloft. These variations give rise to the scintillations noted above.

In addition to changing the direction of travel of an electromagnetic signal and/or causing scintillations, a medium can both extract energy from a signal passing through it and alter the orientation sense of the electric vector (the polarization) of the signal as it passes through. The loss of energy is called *attenuation,* and the change in polarization sense is generally referred to as *depolarization.* In general, the longer the path through a medium is, the greater will be its effect on the electromagnetic signal passing through it. For this reason, paths through the atmosphere at low elevation angles will have greater ray bending, scintillation, attenuation, and depolarization than paths at high elevation angles.

REFRACTIVE EFFECTS

Bulk Refractive Effects

In still air, the atmosphere assumes a spherically stratified form with layers of generally decreasing refractive index lying one above the other. The refractive index of a given portion of the atmosphere will therefore vary far more quickly with change in height than with change in horizontal position. For

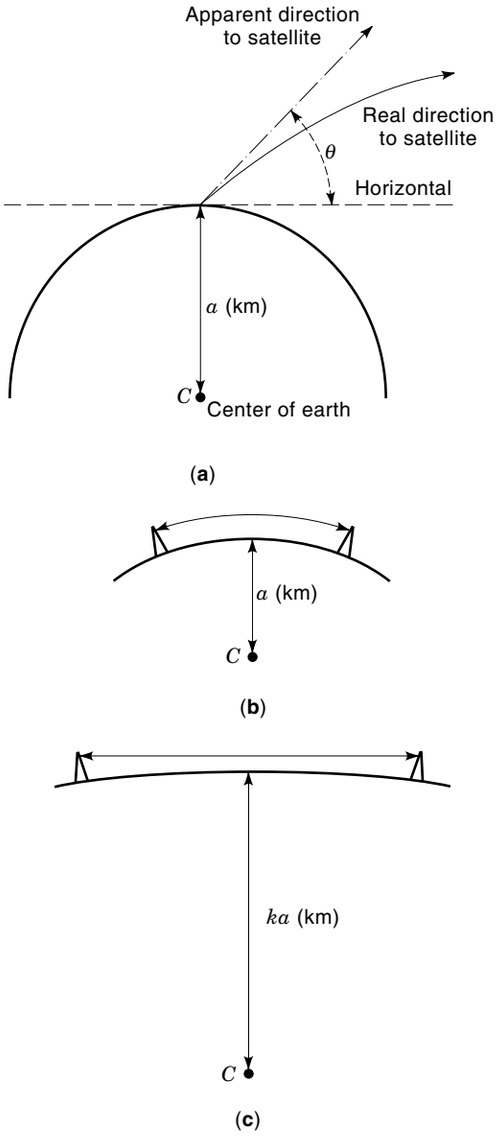

Figure 1. (a) Apparent and real directions to an earth satellite; illustration of methods of ray tracing: (b) real radius and a curved ray path, and (c) effective radius and a geometric ray path.

this reason, an electromagnetic signal (a ray) leaving the surface of the earth at an elevation angle of $<90°$ will bend away from the normal to the surface [see Fig. 1(a)]. The curvature will be contained in one plane, the projection of which onto the surface of the earth is the azimuth direction. If r is the radius of curvature of the ray (2), then

$$\frac{1}{r} = -\frac{\cos\theta}{n}\frac{dn}{dh} \tag{1}$$

where

θ = angle of the ray path to the horizontal at the point considered
n = refractive index of the atmosphere
dn/dh = vertical gradient of refractive index at a height h above the earth's surface

The minus sign indicates that the refractive index decreases with increasing altitude. For terrestrial radio systems, the elevation angle θ will be almost zero, and, since the refractive index is almost unity, Eq. (1) will reduce to the approximate form

$$\frac{1}{r} = -\frac{dn}{dh} \tag{2}$$

If the radius of the earth is a, the difference in curvature between the ray path and the curvature of the earth along the terrestrial link is given by

$$\frac{1}{a} - \frac{1}{r} = \frac{1}{a} + \frac{dn}{dh} = \frac{1}{ka} = \frac{1}{R_e} \tag{3}$$

Here R_e is the effective radius of the earth given by the product ka, where k is the effective earth radius factor. The effective radius of the earth is often used in ray-tracing diagrams of the vertical profiles of terrestrial radio systems, because it allows for the average ray bending along the path [see Fig. 1(b,c)]. Ray bending on satellite-to-ground paths may cause signal loss due to the spreading of the antenna beam. This effect, and that of elevation-angle-of-arrival variations, are negligible at elevation angles above about 3° and will only be significant for large antennas (diameter >100 wavelengths).

The atmosphere has a *dry* and a *wet* refractive index component, the former due to the gases in the atmosphere (principally nitrogen and oxygen), and the latter due to the water vapor that is taken up into the atmosphere. Combining the two components together into a composite refractive index n gives

$$n - 1 = \frac{77.6}{T}\left(P + 4810\frac{e}{T}\right) \times 10^{-6} \tag{4}$$

where

P = atmospheric pressure (hPa)
T = absolute temperature (K)
e = water vapor pressure (hPa)

The hectopascal (hPa) is the same as a millibar.

The water vapor pressure e can be related to the relative humidity by (3)

$$e = He_s/100 \tag{5}$$

and

$$e_s = a\exp\left(\frac{bt}{t+c}\right) \tag{6}$$

where

H = relative humidity (%)
t = temperature (°C)
e_s = saturation vapor pressure (hPa) at the temperature t

and the coefficients a, b, and c are as follows:

For water:

$$a = 6.1121$$
$$b = 17.502$$
$$c = 240.97$$

For ice:

$$a = 6.1115$$
$$b = 22.452$$
$$c = 272.55$$

The vapor pressure e is related to the water vapor density ρ (g/m^3) by (3)

$$e = \frac{\rho T}{216.7} \qquad \text{(hPa)} \tag{7}$$

The refractive index of air is so close to unity that Eq. (4) is often rewritten as

$$n = 1 + 10^{-6}N \tag{8}$$

where N is the *refractivity* of the atmosphere and is given by $(77.6/T)(P + 4810e/T)$, with the same units as in Eq. (4).

Refractivity Profile. The refractivity profile is described by a mean refractive index gradient, which generally decreases exponentially with increasing altitude. A reference standard atmosphere for calculating the refractive index as a function of height, $n(h)$, is given by (3)

$$n(h) = 1 + 10^{-6}N_0 \exp(-h/h_0) \tag{9}$$

where

h = height above mean sea level (km)
h_0 = reference altitude = 7.35 km
N_0 = average value of atmospheric refractivity at mean sea level = 315

Rewriting Eq. (9) in terms of the refractivity, we have

$$N(h) = N_0 \exp(-h/h_0) \tag{10}$$

The rate of change of the refractivity profile with height, dN/dh, can be related to the parameter k used earlier. Sample values are given below (4):

dN/dh (N/km)	k
157	$\frac{1}{2}$
0	1
−40	$\frac{4}{3}$
−157	∞
−200	−3.65

From the table above, it is clear that, when dN/dh is less than −157, the radius of curvature of the earth is greater than the radius of curvature of a signal that is initially propagating horizontal to the surface of the Earth. The signal will therefore propagate beyond what would normally be the local horizon. This is a form of anomalous propagation, and the mechanism is referred to as *ducting*.

Refractive Ducts. Ducting is defined as occurring when a radio ray originating close to the earth's surface is sufficiently refracted that it is either bent back towards the earth's surface or travels along a path that is parallel to the earth's surface. Ducts are formed when layers of air having a relatively high refractive index are above layers with a relatively low refractive index. This *inversion* of the normal exponentially decaying refractive index profile with height is rare and leads to anomalous propagation conditions. Anomalous propagation, and the enhanced signal levels it causes at unlikely distances from the transmitter, is key to the estimation of potential interference between terrestrial systems caused by ducts. A signal will become trapped in a duct if the initial direction of the transmission (the angle of incidence) is very close to that of the horizontal refractive index boundaries of the duct. Typically, the angle of incidence of the signal, as it meets the boundary between the inversion layer and the atmosphere above, has to be smaller for thinner ducts. Typical values for a refractivity gradient of −300 N/km are (2):

Critical Angle of Incidence (deg)	Duct Thickness (m)
0.1	10
0.14	20
0.22	50

Frequency also plays a part in the ducting. The higher the frequency, the smaller the duct thickness consistent with trapping. For the same −300 N/km profile assumed above, the minimum trapping frequency for a surface duct increases approximately from 2 GHz to 2.5 GHz to 4 GHz to 10 GHz to 25 GHz as the duct thickness changes from 40 m to 30 m to 20 m to 10 m, to 5 m, respectively (2). The necessary condition for ducting to occur at a given elevation angle is given by (5)

$$\theta < \theta_c \tag{11}$$

where θ is the elevation angle and θ_c is the critical elevation angle above which ducting will not occur. The critical angle is given by

$$\theta_c = (2|\Delta M|)^{1/2} \qquad \text{(mrad)} \tag{12}$$

where M is the modified refractivity (and $M = N + 10^6\, h/a$, with h the height above the ground and a the radius of the earth), and ΔM is the change in M across the ducting layer. As an example, for θ_c to equal 1°, the required ΔM is 152.3.

Assuming a surface duct 50 m in height, the above M lapse corresponds to a refractivity gradient of 840 N-units/km. Refractivity gradients of this magnitude are extremely rare, and so ducting is normally limited to terrestrial radio systems or satellite-to-ground paths where the elevation angle is below 1°. The latter condition is not expected to be used in commercial systems because it leads to poor propagation, but may have military applications in some situations.

Signal Delay. A signal propagating in the atmosphere will travel at a speed that is less than the speed of light in a vacuum. If a ranging system is being employed, such as the Global Positioning System (GPS), which ignores the true speed of the signal through the atmosphere, an error will be made in calculating the range. There will be two components of range error (here, range *delay,* since the signal will arrive

later than expected). These are the range delay Δ_d due to dry air and the range delay Δ_w due to the moisture in the air. Typical values (6) are given in the table below for a path that exits the atmosphere to a satellite where the refractive index of the atmosphere is assumed to be unity. The range error values have been increased by 2% from those in Ref. 5 to allow for the additional atmosphere encountered from the 80 km height used in Ref. 5 for the target. Regression analyses (7) have shown that these typical range errors can be reduced in practice by 25% by incorporating site latitude, height above sea level, and time of day within the calculation procedure

Initial Elevation Angle (deg)	Elevation Angle Error (mdeg)	Range Error (m)
0	595	106
5	159	25.5
50	13.4	3.2

Small-Scale Refractive Effects

The air is rarely still: differential heating and cooling effects within the atmosphere induce wind currents from balmy breezes to tornado-force hurricanes and tropical cyclones. The resultant turbulence in the troposphere will cause small-scale changes in the refractive index. These in turn will lead to relatively rapid variations in the amplitude, phase, and angle of arrival of a signal (8). The effect on the signal is usually described by one of

1. The log amplitude χ (dB), which equals the ratio of the instantaneous amplitude of the observed signal to its mean amplitude
2. The scintillation variance σ_χ^2 in dB^2 or the intensity σ_χ in dB_{rms}, which are the variance and root mean square of the log amplitude χ, respectively (8)

On terrestrial paths, the turbulence occurs in the *boundary layer*—the part of the troposphere that is next to the surface of the earth. In general, the signal fluctuations due to turbulence on terrestrial paths are neither performance- nor availability-limiting, the major propagation impairments being multipath (due to multiple atmospheric rays and ground reflections) and (for systems operating at frequencies above about 10 GHz) rain attenuation. On earth–space paths, the primary cause of major tropospheric scintillations is cumulus clouds on warm, humid days. The attendant air entrainment process caused by the convective activity within the cloud structure induces turbulence: the more humid and hot the conditions are, the more severe the scintillations become. Similarly, the lower the elevation angle, the larger the amplitudes of both signal enhancements and degradations become. In most systems, tropospheric scintillation will only affect the performance of the link and not its availability (9). At elevation angles below about 5°, however, low-angle fading effects become evident (10,11), and they can be system-limiting (i.e. cause a link outage). Figure 2 illustrates the general concept

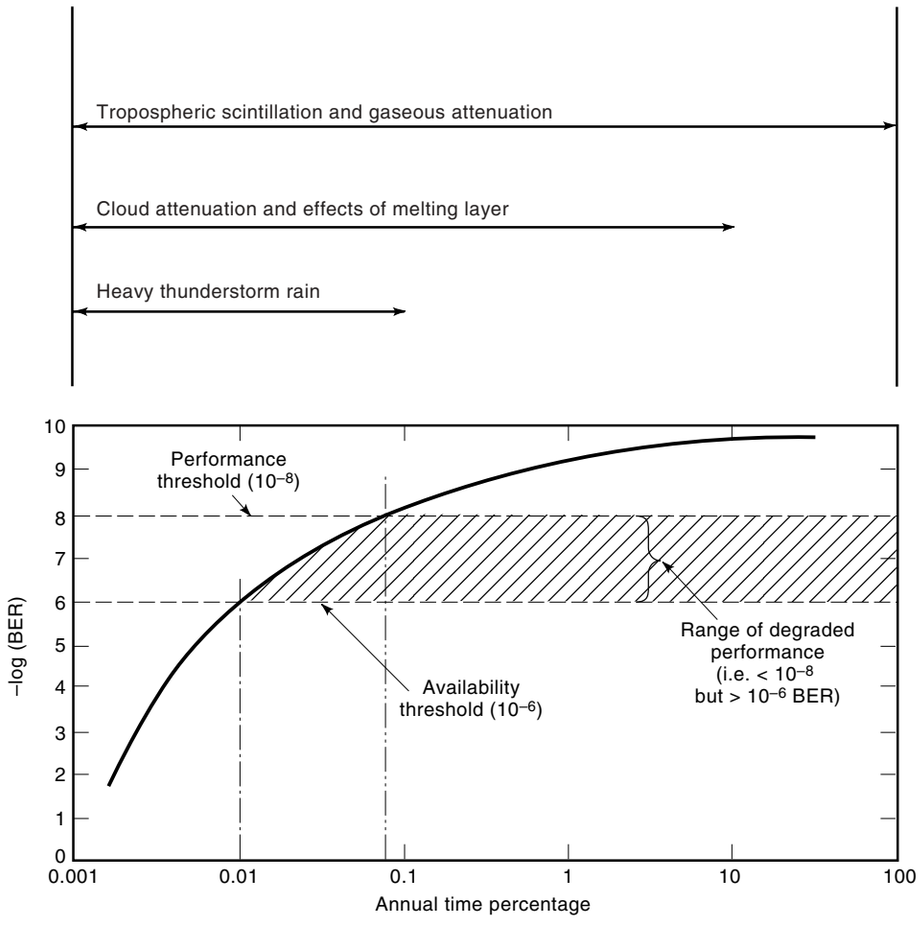

Figure 2. Example of annual statistics of bit error ratio (BER) versus time percentage for a given link.

of performance and availability thresholds for digital communication systems (12).

Prediction of Tropospheric Scintillation

In most systems, it is the probable signal degradation that is required for the link budget analysis (signal enhancements being of relevance only for potential front-end amplifier saturation or for likely interference to other systems). The currently accepted modeling procedure to calculate the effective signal reduction due to tropospheric scintillations on an earth–space path (13) uses the wet term of the refractivity at ground level as the input parameter to predict the scintillation variance. The step-by-step procedure from Ref. 13 is given below for elevation angles $\geq 4°$:

Parameters required for the method include: t = the average surface ambient temperature (°C) at the site for a period of one month or longer; H = average surface relative humidity (%) at the site for a period of one month or longer; f = frequency (GHz), where 4 GHz $\leq f \leq$ 20 GHz; θ = path elevation angle, where $\theta \geq 4°$; D = physical diameter (m) of the earth station antenna; and η = antenna efficiency; if unknown, $\eta = 0.5$ is a conservative estimate.

Step 1. For the value of t, calculate the saturation water vapor pressure, e_s (kPa), as specified in Ref. 3

Step 2. Compute the wet term of the radio refractivity, N_{wet}, corresponding to e_s, t, and H as given in Ref. 3

Step 3. Calculate the standard deviation of the signal amplitude, σ_{ref}, used as a reference:

$$\sigma_{ref} = (3.6 \times 10^{-3}) + (10^{-4} \times N_{wet}) \qquad \text{dB}$$

Step 4. Calculate the effective pathlength L according to

$$L = (2h_L)/\sqrt{\{[\sin^2\theta + 2.35 \times 10^{-4}]^{1/2} + \sin\theta\}} \qquad \text{m}$$

where h_L is the height of the turbulent layer; the value of h_L = 1,000 m

Step 5. Estimate the effective antenna diameter, D_{eff}, from the geometrical diameter, D, and the antenna efficiency, η,

$$D_{eff} = (\eta)^{1/2} D \qquad \text{m}$$

Step 6. Calculate the antenna averaging factor from

$$g(x) = \{[3.86(x^2+1)^{11/12}] \times \sin[(11/6)\arctan(1/x)] - 7.08x^{5/6}\}^{1/2}$$

with

$$x = 1.22(D_{eff})^2(f/L)$$

where f is the carrier frequency in GHz

Step 7. Calculate the standard deviation of the signal for the considered period and propagation path,

$$\sigma = \sigma_{ref}(f)^{7/12}[g(x)/(\sin\theta)^{1.2}]$$

Step 8. Calculate the time percentage factor $a(p)$ from the time percentage, p, of concern in the range $0.01 < p \leq 50$,

$$a(p) = -0.061(\log_{10} p)^3 + 0.072(\log_{10} p)^2 - 1.71\log_{10} p + 3.0$$

Step 9. Calculate the scintillation fade depth for the time percentage p by

$$A_s(p) = a(p)\sigma \qquad \text{dB}$$

The above procedure has been found to predict well at frequencies at least up to 30 GHz, although it tends to underpredict slightly at all frequencies in the hot, humid summer months. At higher frequencies (>30 GHz) it is expected that the same $f^{7/12}$ scaling law will apply as shown in step 7 above, although this anticipated result has not been tested experimentally. The fading portion of the tropospheric scintillation, A_s, is not usually significant for earth-to-space paths at elevation angles above 20° for the frequency bands currently in operation (4 GHz to 30 GHz). As the elevation angle decreases, or the frequency band increases, tropospheric scintillation fading becomes more significant. For example, at 11 GHz, A_s is less than 0.5 dB for 0.01% of an average year at elevation angles on the order of 30°. For the same frequency, A_s approaches 3 dB at elevation angles of 3.2° (11). These values of A_s are for nonraining periods and so will affect the performance of the system.

GASEOUS ABSORPTION

When a molecule or atom is nonsymmetrical in its structure, it will have a preferred orientation if placed in an electric field. Such molecules or atoms are said to be *polar*. Polar molecules or atoms cause far more loss to a radio signal than nonpolar molecules or atoms, since the application of an external field causes the polar molecules or atoms to reorient themselves. The reorientation (or relaxation) of the dipoles will remove energy from the applied field and cause heating of the medium. This is the principle of a microwave oven. The major constituents of the troposphere, oxygen and nitrogen, are electrically nonpolar and so no absorption due to electric dipole resonance will take place. Oxygen however, is a paramagnetic molecule with a permanent magnetic moment which causes resonant absorption at particular frequencies. Water and water vapor, which both contain two oxygen atoms, are therefore polar molecules and so absorption occurs due to resonance at critical frequencies.

Oxygen and Water Vapor Resonance Lines

The specific gaseous attenuation γ (dB/km) is given by

$$\gamma = \gamma_o + \gamma_w \qquad \text{(dB/km)} \tag{13}$$

where γ_o and γ_w are the specific attenuations (dB/km) due to dry air (essentially oxygen) and water vapor, respectively. The specific attenuation needs to be multiplied by the length of the path over which it operates to arrive at total path attenuation. On terrestrial paths, this is simply the distance between the transmitter and receiver, L (km), and the path attenuation A (dB) is given by

$$A = \gamma L = (\gamma_o + \gamma_w)L \qquad \text{(dB)} \tag{14}$$

For earth–space paths, the situation is not so straightforward, since the density and make up of the atmosphere change rapidly with height. The value of L used must be able

to take account of the density and other variations along the link through the atmosphere.

Figure 3, abstracted from Fig. 3 of Ref. 14, gives the total zenith gaseous attenuation at frequencies up to 1 THz (10^{12} Hz) for two conditions: a standard atmosphere and a dry atmosphere. A standard atmosphere is defined as having the following surface characteristics: pressure 1013 hPa, temperature 15°C, and water vapor density 7.5 g/m^3. In general, the dry atmosphere curve in Fig. 3 shows the resonance absorption lines of oxygen, while the standard atmosphere curve is a summation of the resonance absorption lines of water vapor and oxygen. A software code (in Matlab) that calculates the total gaseous attenuation in a line-by-line fashion up to a frequency of 1 THz is available from the Radiocommunication Bureau of the ITU in Geneva.

For nonzenith paths, it is necessary to know not only the specific attenuation at each point in the link but also the length of the path that has this specific attenuation. To derive the incremental path lengths, ray bending through the atmosphere must be considered [see Fig. 1(a)]. A full procedure to accomplish this is given in Ref. 14. In this procedure, formulae are given for the precise calculation of γ_o and γ_w, and the total zenith attenuation is calculated from

$$A_z = \gamma_o h_o + \gamma_w h_w \qquad \text{(dB)} \tag{15}$$

where h_o is the equivalent height of the dry gaseous absorption and h_w is the equivalent height of the water vapor absorption. Typical values of h_o and h_w are 6 km and 2.1 km (during rainy conditions), respectively. For elevation angles between 10° and 90°, a cosecant law gives the total gaseous attenuation A, namely

$$A = \frac{A_z}{\sin\varphi} \qquad \text{(dB)} \tag{16}$$

where φ is the elevation angle. For elevation angles below 10°, a more accurate formula that takes account of the real length of the atmospheric path is required (14). For most earth–space systems, gaseous absorption is not significant compared with the other impairments. It also changes very little with time and so is usually relatively easy to factor into a system design.

RAIN ATTENUATION

Attenuation due to rain is made up of two components: absorption and scattering. Absorption takes place when the incident signal energy is transformed into mechanical energy, thereby heating the raindrop. Scattering occurs when the incident signal is redirected away from the desired propagation path without energy loss to the raindrop. The relative importance of scattering and absorption is a function of the complex index of refraction of the raindrop and the size of the raindrop relative to the wavelength of the signal (15). The significance of the scattered component generally increases both with the signal frequency and with the size of the raindrop. In general, attenuation due to rain increases with increasing signal frequency for a given rain rate. Typical annual cumulative statistics for frequencies of 12 GHz, 18.7 GHz, 39.6 GHz, and 49.5 GHz on paths at an elevation angle of approximately 38° in Europe are shown in Fig. 4 (some data were extracted from Ref. 16). These curves show a monotonic increase in attenuation with decreasing time percentage, which is typical of temperate climates. There is evidence, however, that in tropical, high-rain-rate regions there is a saturation effect in the attenuation and rainfall rate statistics at low time percentages, leading to a breakpoint in the cumulative statistics (17). This and other features of high-rain-rate regions make the accurate prediction of attenuation due to rain very difficult for those locations.

Rain does not usually consist of a homogeneous collection of raindrops falling at a constant rate. The size, shape, temperature, and fall velocities usually vary in a dynamic manner along the path. To calculate the attenuation of a radio signal passing through rain it is necessary to invoke a drop-size distribution and to integrate the attenuation contributions of the various raindrops along the path through the rain. The characteristics of rain vary so much in space and

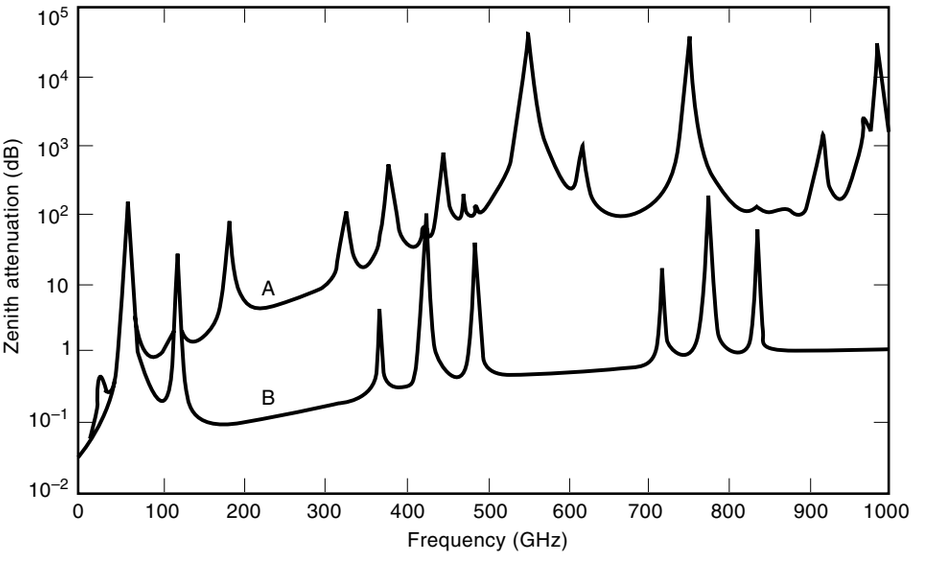

Figure 3. Zenith attenuation due to atmospheric gases (from Fig. 3 of Ref. 14). Curve A: standard atmosphere (7.5 g/m^3); curve B: dry atmosphere. © ITU. Reproduced with permission.

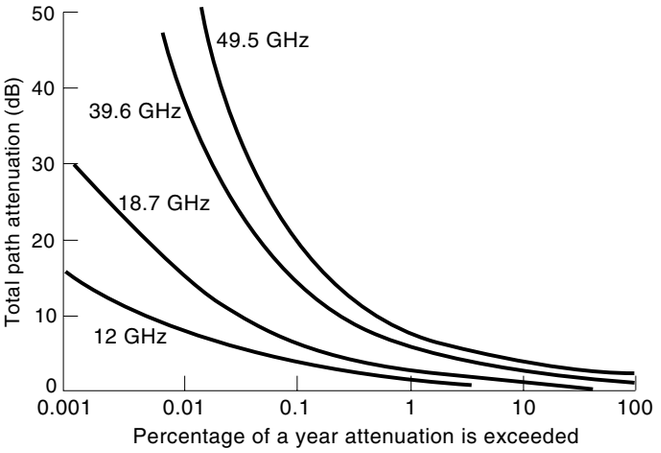

Figure 4. Average annual cumulative statistics of total path attenuation at an elevation angle of about 38° in Europe (some data extracted from Ref. 16).

time that it is necessary to resort to empirical methods that employ statistical averaging. The accepted approach is to use a power law representation based on the rainfall rate R (usually a rainfall rate measured at a point on the ground close to the communications link). The specific attenuation γ (dB/km) in rain is related to the rainfall rate R (mm/h) by the power law relationship

$$\gamma = kR^{\alpha} \qquad \text{(dB/km)} \tag{17}$$

where k and α are regression coefficients (18) that take account of absorption and scattering.

Prediction of Attenuation

Rain-attenuation prediction models fall into two classes: (1) those that attempt to analyze the physics of the process and model the constituents of storm cells, and so on; and (2) those that use empirical approaches with simplified assumptions. To date, those that use empirical methods have demonstrated the most consistent accuracy on a global basis (although, with the strong emphasis currently on the development of accurate, world-wide climatic parameter maps, a physical modeling approach should eventually prevail). For empirical methods, the key to the prediction process is the development of a procedure that enables the user to move seamlessly from point rainfall rate on the ground to average rainfall rate along the path at any elevation angle. This approach is described below, abstracting directly from the current ITU-R prediction procedure for calculating rain attenuation on a satellite-to-ground path, as set out in Ref. 13:

The following parameters are required: $R_{0.01}$ = point rainfall rate for the location for 0.01% of an average year (mm/h); h_s = height above mean sea level of the earth station (km); θ = elevation angle; f = frequency (GHz). The geometry is illustrated in Fig. 5. The method is applicable up to at least 30 GHz.

Step 1. Calculate the effective rain height, h_R, for the latitude of the station, ϕ:

$$h_R\ (\text{km}) = \begin{cases} 5 - 0.075(\phi - 23) & \text{for } \phi > 23^\circ \text{ Northern Hemisphere} \\ 5 & \text{for } 0^\circ \le \phi \le 23^\circ \text{ Northern Hemisphere} \\ 5 & \text{for } 0^\circ \ge \phi \ge -23^\circ \text{ Southern Hemisphere} \\ 5 + 0.1(\phi + 21) & \text{for } -71^\circ \le \phi < -21^\circ \text{ Southern Hemisphere} \\ 0 & \text{for } \phi < -71^\circ \text{ Southern Hemisphere} \end{cases}$$

Step 2. For $\theta \ge 5°$ compute the slant-path length, L_s, below the rain height from:

$$L_s = (h_R - h_S)/(\sin\theta) \qquad \text{km}$$

For $\theta < 5°$, the following formula is used:

$$L_s = [2(h_R - h_S)]/\{[\sin^2\theta + 2(h_R - h_S)/8500]^{1/2} + \sin\theta\} \qquad \text{km}$$

Step 3. Calculate the horizontal projection, L_G, of the slant-path length from:

$$L_G = L_S \cos\theta \qquad \text{km}$$

Step 4. Obtain the rain intensity, $R_{0.01}$, exceeded for 0.01% of an average year at the site

Step 5. Calculate the reduction factor, $r_{0.01}$, for 0.01% of the time for $R_{0.01} \le 100$ mm/h

$$r_{0.01} = 1/(1 + L_G/L_0)$$

where $L_0 = 35 \exp(-0.015\, R_{0.01})$ and, for $R_{0.01} > 100$ mm/h, use the value 100 mm/h in place of $R_{0.01}$.

Step 6. Obtain the specific attenuation, γ_R, using the frequency dependent regression coefficients k and α [Ref. 18] by using

$$\gamma_R = k(R_{0.01})^{\alpha} \qquad \text{dB/km}$$

Step 7. The predicted attenuation exceeded for 0.01% of an average year is obtained from

$$A_{0.01} = \gamma_R L_S r_{0.01} \qquad \text{dB}$$

Step 8. The estimated attenuation to be exceeded for other percentages of an average year, in the range 0.001% to 1%, is de-

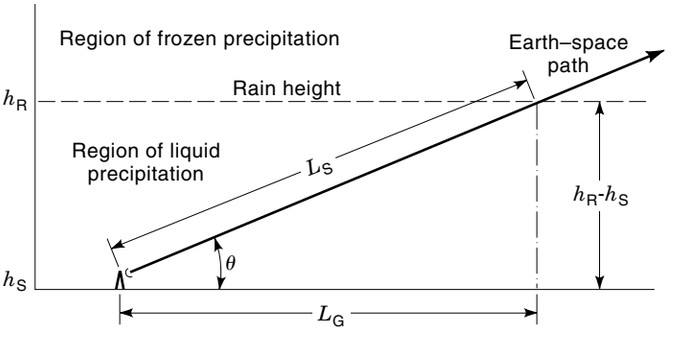

Figure 5. Schematic presentation of earth–space path (from Fig. 1 in Ref. 13). © ITU. Reproduced with permission.

termined from the attenuation exceeded for 0.01% of an average year by using

$$(A_p)/(A_{0.01}) = 0.12p^{-(0.546+0.043\log p)}$$

Note that the variability of the weather from year to year will cause this prediction method to vary similarly. Average accuracy better than about 35% should not be expected for any given year.

DEPOLARIZATION

The polarization sense of a wave usually refers to the preferred orientation of the electric vector. A perfectly polarized wave will have no component of its electric field in the orthogonal sense. There are only two states for a perfectly polarized wave: linear and circular. For linear polarization, it is common to use vertical and horizontal as the two orthogonal (linear) reference axes. For circular polarization, right-hand circular polarization (RHCP) and left-hand circular polarization (LHCP) are the two orthogonal (circular) reference senses. Depolarization from one reference polarization sense to the other occurs when the signal passes through an anisotropic medium and the polarization sense of the signal is not aligned with the principal axes of the medium. Rain can be such a medium.

Raindrops exist in a dynamic medium: the atmosphere. When the drops are very small, surface tension forces (which strive to keep the drop perfectly spherical) far exceed the aerodynamic forces on the raindrop (which seek to shape the drop to conform with the external pressures). Under these conditions, the raindrops remain spherical and the rain medium appears symmetrical to the signal. No signal depolarization therefore results. As the drops become larger, however, through coalescence with other drops on collision in the rain medium, the surface tension forces can no longer keep the drops spherical. The drops distort into elliptical shapes and so exhibit preferred orientation directions along the major and minor axes of the ellipsoid. Differential attenuation and phase shift will occur on component signals propagating along these axes and will result in signal depolarization. The degree of depolarization measured is called the *cross-polarization discrimination* (XPD) and is defined as

$$\mathrm{XPD} = 20\log_{10}\frac{E_{\mathrm{co}}}{E_{\mathrm{cross}}} \qquad \text{(dB)} \tag{18}$$

where E_{co} is the field measured in the wanted (copolarized) polarization and E_{cross} is the field measured in the unwanted (cross-polarized) polarization. If the differential attenuation (α, nepers) and differential phase (β, radians) caused by a medium are known, XPD can be calculated from

$$\mathrm{XPD} = 20\log_{10}\left|\frac{e^{-(\alpha+j\beta)}+1}{e^{-(\alpha+j\beta)}-1}\right| \qquad \text{(dB)} \tag{19}$$

Generally α and β are not known, and it is usual to model XPD against rain attenuation.

Prediction of Cross-Polarization Discrimination

The most often used prediction method for calculating XPD is that in the ITU-R Recommendation 618 (13). The procedure is abstracted directly below:

The following parameters are needed: A_{p}, the rain attenuation (dB) exceeded for the required percentage of time, p, for the path in question; τ = tilt angle of the linearly polarized electric field with respect to the horizontal (for circular polarization use τ = 45°); f = frequency (GHz); θ = path elevation angle (degrees). The method is applicable to frequencies between 8 GHz and 35 GHz.

Step 1. Calculate the frequency-dependent term

$$C_f = 30\log(f) \qquad \text{for} \quad 8 \le f \le 35\,\mathrm{GHz}$$

Step 2. Calculate the rain attenuation dependent term

$$C_A = V(f)\log A_{\mathrm{p}}$$

where

$$V(f) = 12.8f^{0.19} \qquad \text{for} \quad 8 \le f \le 20\,\mathrm{GHz}$$
$$V(f) = 22.6 \qquad \text{for} \quad 20 < f \le 35\,\mathrm{GHz}$$

Step 3. Calculate the polarization improvement factor

$$C_\tau = -10\log[1 - 0.484(1+\cos 4\tau)]$$

The improvement factor $C_\tau = 0$ for $\tau = 45°$ (which is equivalent to circular polarization) and reaches a maximum value of 15 dB for linearly polarized signals with $\tau = 0°$ or 90°.

Step 4. Calculate the elevation angle dependent term

$$C_\theta = -40\log(\cos\theta) \qquad \text{for} \quad \theta \le 60°$$

Step 5. Calculate the canting angle dependent term

$$C_\sigma = 0.0052\sigma^2$$

σ is the effective standard deviation of the raindrop canting angle distribution, expressed in degrees; σ takes the value 0°, 5°, 10°, and 15° for 1%, 0.1%, and 0.01%, and 0.001% of the time, respectively.

Step 6. Calculate the rain XPD not exceeded for p% of the time:

$$\mathrm{XPD}_{\mathrm{rain}} = C_{\mathrm{f}} - C_{\mathrm{A}} + C_\tau + C_\theta + C_\sigma \qquad \mathrm{dB}$$

Step 7. Calculate the ice crystal dependent term

$$C_{\mathrm{ice}} = \mathrm{XPD}_{\mathrm{rain}} \times [(0.3 + 0.1\log p)/2] \qquad \mathrm{dB}$$

Step 8. Calculate the XPD not exceeded for p% of the time, including the effects of ice crystals:

$$\mathrm{XPD}_{\mathrm{p}} = \mathrm{XPD}_{\mathrm{rain}} - C_{\mathrm{ice}} \qquad \mathrm{dB}$$

For frequencies below 8 GHz the scaling formula below can be used for $4 \le f_1, f_2 \le 30$ GHz:

$$\mathrm{XPD}_2 = \mathrm{XPD}_1 - 20\log\frac{f_2[1 - 0.484(1+\cos 4\tau_2)]^{1/2}}{f_1[1 - 0.484(1+\cos 4\tau_1)]^{1/2}}$$

The component for ice depolarization in the above formulation, C_{ice}, is known to underestimate the degree of ice crystal depolarization encountered on low-elevation-angle paths.

Depolarization can be system-limiting in the lower frequency bands, where rain attenuation is not significant (e.g., in the C band, which is the 6/4 GHz uplink–downlink pair for many satellite systems). As the frequency goes up, however, the amount of depolarization observed per decibel of at-

tenuation becomes less and less until, by Ka band (the 30/20 GHz uplink–downlink pair), depolarization is rarely system-limiting. In analog systems, an XPD margin of 12 dB is usually required to operate successfully. In digital systems, this margin can be reduced due to the possibility of adding coding to the signal. When two satellite links are sharing the same transponder, but are using opposite polarizations (this is referred to as polarization frequency reuse), depolarization caused by ice crystals can be a problem. This is because the unwanted (depolarized) component of one link caused by the ice crystals will enter the channel of the wanted signal in the satellite transponder without any attenuation having occurred.

ATTENUATION DUE TO CLOUDS AND FOG

Fog or mist is essentially supersaturated air in which some of the water has precipitated out to form small droplets of water, usually ≤ 0.1 mm in diameter (19). Fog is mainly formed from two processes—radiation and advection (6)—and rarely extends more than 100 m above the ground. For this reason, fog is usually ignored in satellite-to-ground link design for frequencies below about 100 GHz. Clouds, however, are much more complicated.

Several models are available for the prediction of cloud attenuation (19–23), but there remain two major difficulties in turning these into link design tools: (1) an accurate cumulative distribution of the vertical and horizontal extent, on a global basis, of those clouds that contribute to slant-path attenuation; and (2) separating this attenuation contribution from that due to rain formed in some of the cloud processes. Many measurements of rain attenuation implicitly include attenuation due to clouds. Understanding, and accurately predicting, the contribution of clouds to path attenuation is a key element in the modeling of the proposed V-band (50/40 GHz) satellite services. Of equal importance will be the development of modeling procedures that can predict the combined effects of all the attenuating phenomena on an earth–space link (24,25).

ATTENUATION EFFECTS ON INFRARED AND VISIBLE LIGHT

The far infrared (~1 THz), infrared (~10 THz), and visible (~100 THz) portions of the electromagnetic spectrum have been utilized for many applications. Figure 3 shows that, for a dry atmosphere, the total zenith attenuation is only about 1 dB at 1 THz. This value of zenith attenuation is fairly constant for frequencies through visible light (100 THz). A "window" in the standard atmosphere exists around 890 GHz, the frequency of HCN masers, but the zenith attenuation at this frequency is still two orders of magnitude higher than that in the dry atmosphere (i.e., 100 dB versus 1 dB total zenith attenuation). For all three frequency ranges, the key attenuating elements in the atmosphere are aerosols, usually cloud and fog droplets. Thick fog (liquid water density ≈ 0.5 g/m^3) will cut visibility to 50 m (19). Most free-space laser links are therefore short-range (<1 km) unless extraordinary powers are contemplated, such as the ~1 MW chemical oxygen iodine laser (COIL) lasers planned for missile interception. At such huge power levels, though, the almost instantaneous heating process caused by the passage of the beam through the atmosphere will modify the constituents along the path, thereby altering the transmission characteristics significantly.

BIBLIOGRAPHY

1. J. Powers, *An Introduction to Fiber Optic Systems,* 2nd ed., Homewood, IL: Irwin, 1997, Chap. 2, Sec. 2.2.
2. Effects of tropospheric refraction on radiowave propagation, Rec. ITU-R P.834-2, *ITU-R Recommendations, Propagation in Ionized and Non-ionized Media,* 1997.
3. The radio refractive index: Its formula and refractivity data, Rec. ITU-R P.453-6, *ITU-R Recommendations, Propagation in Ionized and Non-ionized Media,* 1997.
4. M. P. M. Hall and C. M. Comer, Statistics of tropospheric radio-refractive index soundings taken over a three year period in the UK, *Proc. IEE,* **116**: 685–690, 1969.
5. H. T. Dougherty and B. A. Hart, Recent progress in duct propagation predictions, *IEEE Trans. Antennas Propag.,* **27**: 542–548, 1979.
6. W. L. Flock, Propagation effects on satellite systems at frequencies below 10 GHz, NASA Reference Publication 1108, 1983.
7. E. E. Altshuler, Tropospheric range-error corrections for the Global Positioning System, *IEEE Trans. Antennas Propag.,* **46**: 643–649, 1998.
8. D. Vanhoenacker-Janvier, Review of tropospheric scintillation measurements and prediction techniques, *CLIMPARA'98, Proc. URSI Commission F Open Symp. on Climatic Parameters in Radiowave Propagation Prediction,* Ottawa, Canada, 1998, pp. 93–98.
9. E. T. Salonen, J. K. Tervonen, and W. J. Vogel, Scintillation effects on total fade distribution for earth–satellite links, *IEEE Trans. Antennas Propag.,* **44**: 23–27, 1996.
10. J. L. Strickland, R. L. Olsen, and H. L. Werstiuk, Measurement of low-angle fading in the Canadian Arctic, *Ann. Telecommun.* **32**: 530–535, 1977.
11. D. L. Bryant, Low elevation angle 11 GHz beacon measurements at Goonhilly earth station, *BT Technol. J.,* **10** (4): 68–75, 1992.
12. J. E. Allnutt and A. W. Dissanayake, The combination of attenuating phenomena in prediction procedures for 10–50 GHz satellite-to-ground paths, *CLIMPARA'98, Proc. URSI Commission F Open Symp. Climatic Parameters Radiowave Propagation Prediction,* Ottawa, Canada, 1998, pp. 183–190.
13. Propagation data and prediction methods required for the design of earth–space telecommunications systems, Rec. ITU-R P.618-5, *ITU-R Recommendations, Propagation in Ionized and Non-ionized Media,* 1997.
14. Attenuation by atmospheric gases, Rec. ITU-R P.676-3, *ITU-R Recommendations, Propagation in Ionized and Non-ionized Media,* 1997.
15. G. Brussaard, Radiometry: A useful tool? ESA publication SP-1071, 1985.
16. R. Polonio and C. Riva, ITALSAT propagation experiment at 18.7, 39.6, and 49.5 GHz at Spino D'Adda: Three years of CPA statistics, *IEEE Trans. Antennas Propag.,* **46** (5): 631–642, 1998.
17. G. H. Bryant, The structure of tropical rain from attenuation and rain exceedences, *Proc. ISAP'92,* Sapporo, Japan, 1992, pp. 877–880.
18. Specific attenuation model for rain for use in prediction methods, Rec. ITU-R P.838, *ITU-R Recommendations, Propagation in Ionized and Non-ionized Media,* 1992.
19. Attenuation due to clouds and fog, Rec. ITU-R P.840-2, *ITU-R Recommendations, Propagation in Ionized and Non-ionized Media,* 1997.

20. D. S. Slobin, Microwave noise temperature and attenuation of clouds: Statistics of these effects at various sites in the United States, Alaska, and Hawaii, *Radio Sci.,* **17**: 1443–1454, 1987.
21. E. E. Altshuler and R. A. Marr, Cloud attenuation at millimeter wavelengths, *IEEE Trans. Antennas Propag.,* **37**: 1473–1479, 1989.
22. F. Dintelmann and G. Ortgies, A semi-empirical model for cloud attenuation prediction, *Electron. Lett.,* **25**: 1487–1488, 1989.
23. E. Salonen, Prediction models of atmospheric gases and clouds for slant path attenuation, *Olympus Utilization Conf.,* Seville, Spain, 1993, pp. 615–622.
24. G. Feldhake, Estimating the attenuation due to combined atmospheric effects on modern earth–space paths, *IEEE Antennas Propag. Mag.,* **39**: 26–34, 1997.
25. A. W. Dissanayake, J. E. Allnutt, and F. Haidara, A prediction model that combines rain attenuation and other propagation impairments along earth–space paths, *IEEE Trans. Antennas Propag.,* **45**: 1546–1558, 1997.

JEREMY E. ALLNUTT
Virginia Tech/Northern Virginia Center

REFRACTION CAUSED BY ILLUMINATION. See PHOTOREFRACTIVE EFFECT.

REGULATORS, SELF-TUNING. See SELF-TUNING REGULATORS.

REJECTION. See TESTING FOR ACCEPTANCE-REJECTION.